Supplementary Materials for

**Herbivores as drivers of negative density dependence
in tropical forest saplings**

Dale L. Forrister*, María-José Endara, Gordon C. Younkin,
Phyllis D. Coley, Thomas A. Kursar

*Corresponding author. Email: dale.forrister@utah.edu

This PDF file includes:

Materials and Methods:

Study Site and Data Collection:

This analysis was conducted using data from the 50-ha forest dynamics plot on Barro Colorado Island, Panama (9° 09' N, 79° 50'W). The plot receives 2,600 mm rain per year, and has a pronounced 3.5-month dry season from January to April (*44*). Complete censuses have been conducted in 1981-1983, and in five-year intervals from 1985 to 2015 (*45–48*). Data from all eight censuses were used in this analysis. In each census, all free-standing trees and shrubs >1 cm diameter at breast height (1.3 m) were mapped, identified to species, and the diameter at breast height (dbh) measured, providing data on growth and survival for over 423,000 trees.

Sampling and quantification of *Inga* traits:

Resource acquisition traits for our nine focal species were taken from (*32, 49*) and include:

1.   *Wood density:* SG60C_AVG – mean wood specific gravity after drying at 60°C (g cm^{-3}) and SG100C_AVG – mean wood density after drying at 100°C (g cm^{-3}).

2.   *Leaf Morphology:* LEAFAREA_AVD – mean leaf area (cm^2) for leaves receiving direct sunlight, LMALEAF_AVD – mean leaf mass per unit area measured for the entire leaf including the petiole (g m^{-2}) for leaves receiving direct sunlight, LEAFTHCK_AVD – mean leaf lamina thickness (mu) for leaves receiving direct sunlight, LMADISC_AVD – mean leaf mass per unit area measured for a 1.483 cm^2 leaf disc taken to avoid veins (g m^{-2}) for leaves receiving direct sunlight, LMALEAF_AVD – mean leaf mass per unit area measured for the entire leaf including the petiole (g m^{-2}) for leaves receiving direct sunlight, LDDISC_AVD – mean leaf tissue density (g cm^{-3}) for leaves receiving direct

sunlight, LDMC_AVD – mean leaf dry matter content (g g^{-1}) for leaves receiving direct sunlight.

3. *Tree Height:* DBH_AVG – mean dbh measured in 2005 of up to the six largest individuals in the BCI 50-ha plot (mm), HEIGHT_AVG – mean height of up to the six largest individuals in the BCI 50-ha plot (m), DIAM_AVG – mean crown diameter of up to the six largest individuals in the BCI 50-ha plot (m).

4. *Leaf Elemental Composition:* The following elemental parameters were quantified in the leaves of each species: amount per dry weight of Al, Ca, Cu, K, Mg, Mn, P, Zn, C and N and the stable isotope compositions, ^{13}C and ^{15}N.

We measured a total of five defensive traits that capture the entire defensive profile of each species. These were measured only on expanding leaves because more than 80% of the damage accrued during a leaf´s lifetime happens during the short period (1-3 weeks) of leaf expansion (reviewed in *17*). This set of defense traits includes:

1. *Developmental defenses:* Leaf expansion rate was determined as the percent increase in area per day. Chloroplast development was measured as the chlorophyll content (mg dm^{-2}) of leaves between 30% and 80% of full expansion.

2. *Biotic defenses: Inga* leaves have extrafloral nectaries that produce nectar and attract protective ants only during the short period of leaf expansion. We quantified the diameter of these nectaries and the abundance of ants visiting them (# of ants per nectary).

3. *Leafing phenology:* The timing and within-population synchrony of new leaf production serve as a defense against herbivory (*50, 51*). We monitored 50 individuals per species on a monthly basis for the presence and absence of new leaves from March 2001 to

November of 2004. We employed circular statistics to analyze the distribution of leaf

flushing throughout the year (*52*). We calculated a pairwise Pearson correlation between

each species using the R package *circular* (*53*).

4. *Hairs*: Some *Inga* species have non-glandular trichomes (hairs) on the leaf surface and

    veins that provide a physical defense, particularly against early instar caterpillars (*54*).

    We measured the density (#/0.01 in^2) and length (mm) of the trichomes on the top and

    bottom leaf-lamina and primary veins.

5. *Chemical defenses: Inga* species invest approximately 45% of dry weight in soluble

    secondary metabolites that play a key defensive role against herbivore attack (*17, 26, 27,*

    55). In this analysis, we focused on intermediate polarity compounds, which are primarily

    phenolic and saponin small molecules. Expanding leaves were dried in the field over

    silica at ambient temperature. The chemical defensive profile for each species was

    determined using untargeted metabolomics following the protocol of (*55*. See

    Metabolomic analysis section below for detailed methods).

Standardization of trait values and dimensionality reduction:

In order to reduce the number of variables measured per trait into a usable value for trait

similarity, we calculated the Mahalanobis distance between species (*56*) for each trait. The

Mahalanobis distance simultaneously controls for correlations between measurements and allows

for different numbers of measurements for each trait, which varied from two to 13. First, all

measured variables for a given trait were projected and scaled into principal component space.

The Mahalanobis distance between a pair of species is the Euclidean distance in principal

component space between those two species. Pairwise trait distance matrices were then

calculated for each trait and normalized between 0 and 1 by dividing each value in the matrix by

the maximum paired distance. Finally, we converted the pairwise distance matrix into a similarity matrix (similarity = 1 – distance) in order to simplify model interpretations.

<u>Metabolomic analyses:</u>

1.   *Sample extraction and data processing:*

Samples were extracted with 44.4 mM ammonium acetate (pH 4.8) : acetonitrile, 60:40, v/v as described in (*55*). Soluble metabolites were analyzed by ultra-performance liquid chromatography coupled to mass spectrometry (UPLC-MS) using an Acquity UPLC I-Class system and a Xevo G2 Q-ToF spectrometer equipped with LockSpray and an electrospray ionization source (Waters, Milford, MA, USA). Data were collected in negative ionization mode.

The MS conditions were as follows: capillary voltage 2.50 kV, sampling cone voltage 45 V, extraction cone voltage 3.5 V, source temperature 100°C, desolvation gas temperature 400°C, desolvation gas flow 600 L/h, negative ionization and resolution modes, *m/z* (mass to charge) ratio of 50–2000 Da, centroid mode, and a collision energy of 6 eV. In MS mode, the collision energy is set by the manufacturer (not user-controlled) and functions to enhance sensitivity and resolution while avoiding fragmentation.

Raw data from the UPLC-MS analysis were processed for peak detection, peak alignment and peak filtering using MassLynx (Waters) and the R package XCMS (*57*) as described in (*55*) except that the parameters used were: feature detection method 'findChromPeaks' (ppm=15, peakwidth=c(4,12), snthresh=5, prefilter=c(10,500)); peak grouping method 'groupChromPeaks' (bw=3, binSize=0.025, minSamples=1, minFraction=0.01); retention time correction method 'Obiwarp' (binSize=1); and integrate areas of missing peaks method 'fillChromPeaks' (expandMZ=0.25,

expandRt=0.5). XCMS processing was performed for each species independently, with five leaf samples included as replicates. The results obtained by XCMS were post-processed in the R package CAMERA to assign the various ions and termed features, that are derived from one compound to that compound (*58*). This uses a defined set of rules for linking the precursor ion with adducts and neutral losses (*59*). The parameters used were: peak grouping after retention time '*groupFWHM*' (perfwhm: 0.7); annotate isotopes '*findIsotopes*'; verify grouping '*groupCorr*'(cor_eic_th=0.5, pval=0.5, graphMethod="lpc", calcIso=TRUE, calcCis=TRUE, calcCas=TRUE); and annotate adducts '*findAdducts*' (polarity='negative'). In addition, peaks eluting before 1 minute or after 32 minutes and peaks at least 1/3 as abundant in the blank runs as in the sample runs were removed from the analysis.

2. *Fast Data Dependent Acquisition (DDA) and MS/MS for abundant compounds:*

Fast Data Dependent Acquisition (DDA), which automatically detects peaks and collects MS/MS spectra for selected ions, was used to collect MS/MS spectra for about 70% of the abundant compounds. Two samples per species were analyzed via Fast DDA, and the MS/MS spectra collected were matched to peaks identified by XCMS in R. In cases where a compound was present in at least one sample with a total ion current (TIC) value of 5000 or greater, but an MS/MS spectrum was not collected during Fast DDA, spectra were collected using the MSMS function.

DDA conditions were as follows. MS Survey: range 30-2000 Da, switching threshold 'Intensity of individual ion rising above' 5000 intensity sec^{-1}, MS scan time 0.5 sec, centroid mode; MS/MS: maximum 5 ions selected for MS/MS from a single MS survey scan, MS/MS scan time 0.5 sec, centroid mode, stop MS/MS when BPI falls

below 5000 intensity sec^{-1} or switch off after 5 seconds have elapsed; Peak Detection: 'Apply no criteria other than intensity'; Exclude: real time exclusion of masses from MS/MS acquire and then exclude for 10 sec; Collision Energy (CE): use collision energy ramp, Low Mass CE Ramp 10-30 V, High Mass CE Ramp 50-100 V. MSMS conditions were similar but used a 2 second scan time.

3. *Compound matching across species:*

In the Python programming language, peaks identified by XCMS were compared between species and matched based on *m/z* and retention time (https://github.com/ColeyKursarLab/endara_sawflies_2018). Individual chromatographic features were matched across samples using a mass tolerance of 0.01 Da and a retention time tolerance of 20s. Compounds were also matched across samples by calculating a cosine similarity score between the associated chromatographic features, which takes into account both the presence and relative TIC values of the features. To calculate the cosine score between two compounds, the set of features associated with each compound is represented as a vector, and the cosine score between the vectors in multidimensional space is calculated. Compounds are considered to be the same if they receive a score of at least 0.5. This results in a comprehensive list of all compounds found in all samples and the relative abundances of each of their associated chromatographic features. In order to ensure that even low-abundance compounds were detected, the function '*getPeaks*'(step=0.05) from the R package XCMS was used to search for all identified chromatographic features in each sample. When searching for features, we used a *m/z* tolerance of 25 ppm and a retention time tolerance of 30 seconds, and features were required to be at least five times more abundant than the same feature found in the

associated blank. In order to filter out noise, features were removed from the analysis if the peak area was less than 1000 or if signal was not above zero in at least seven consecutive scans.

With the resulting list of chromatographic features and their abundances in each sample, the presence and abundance of each compound in each sample was calculated. A sample was said to contain a compound if it contained all features that were at least three quarters as abundant as the most abundant feature in that compound. The abundance of a compound was calculated by summing the TIC of all chromatographic features associated with that compound.

4. *Select a single MS/MS spectrum for each compound:*

Many compounds were associated with multiple MS/MS spectra, either as a result of spectra being collected from multiple chromatographic features (adduct ions, isotopic homolog ions, etc.), or because the same compound was present in multiple *Inga* species. In the case where spectra were collected for multiple chromatographic features, the spectrum associated with the most abundant feature was used. In the case where spectra were collected from the same compound in multiple species, the spectrum with the highest signal was used.

5. *Chemical Similarity Calculations:*

A molecular network was created for all compounds for which MS/MS spectra were obtained by uploading an mgf file to Global Natural Products Social Molecular Networking (GNPS, https://gnps.ucsd.edu/ProteoSAFe/static/gnps-splash.jsp; (*60*)) with the following parameters: precursor ion mass tolerance: 0.02 Da, fragment ion mass tolerance: 0.02 Da, min pair cos: 0.5, network topK: 1000, maximum connected

component size: 0, minimum matched fragment ions: 6, minimum cluster size: 1, run

MSCluster: no. In the resulting network, structurally similar compounds are assigned a

similarity score ranging from 0 (completely dissimilar) to 1 (identical) based on the

similarity of their MS/MS fragmentation spectra. These networks were downloaded from

GNPS and loaded into R.

A similarity value for each sample pair was calculated using the chemical

structural and compositional similarity index described in (*61*). This index requires a

compound-by-compound similarity matrix using compound similarity scores from

GNPS, and a compound-by-sample matrix with the abundance of each compound in each

sample. Compound abundance was approximated using the TIC of the chromatographic

peak. Abundances were normalized within each sample such that total abundance of any

given sample was equal to 1.0. The resulting sample-by-sample matrix was converted to

the species-by-species similarity matrix used in the trait analysis by averaging the

chemical structural and compositional similarity values for all sample pairs of each

species pair.

Herbivore host associations:

To record host associations of lepidopteran herbivores, we visually searched young leaf

flushes on saplings of the focal tree species and collected only those larvae that were found

feeding. Insects were collected by hand from the leaves by three researchers in 2012 for a period

of 2 months. All caterpillars were assigned to morphospecies in the field. Because no

identification keys to the caterpillars of this region exist, all herbivores were subsequently

assigned to molecular operational taxonomic units (MOTUs) on the basis of DNA barcode

sequences for the mitochondrial gene, cytochrome oxidase I (COI) (see below). We recorded a

total of 613 individuals in 55 MOTUs from 24 families of Lepidoptera.

PCR amplification and DNA sequencing for most of our samples were generated at the Canadian Center for Barcoding using standard barcoding protocols (*62, 63*). The sequences were assembled into contigs and manually edited using the program Sequencer version 5.1 (Gene, Codes). The resulting sequences were subsequently aligned using the program MUSCLE (*64*).

MOTU assignment used COI sequence data and the software package jMOTU (*65*), with a similarity cutoff of 15 bp ($^\sim$2.3%). MOTUs identified using Automatic Barcode Gap Discovery (ABGD) (*66*) were identical. MOTUs were allocated to taxonomic families by BLASTing each consensus sequence against the NCBI BLAST web interface, with a minimum accepted similarity for family assignment of 90% (Figure S2).

We then quantified the similarity in herbivore community between *Inga* species using the Jaccard similarity in the R Package *vegan* (*67*). This similarity measures quantifies compositional similarity in herbivore MOTUs weighted by the abundance of each MOTU observed feeding on each species.

Quantifying the impact of neighborhood similarity on growth and survival:

All individuals from the nine focal *Inga* species within the 50-hectare plot that were more than 10 meters from the plot edge were used as focal trees in this analysis, including those for which no conspecific or congeneric were present within 10 meters. For each focal tree and for each trait category, a neighborhood similarity was calculated using Equation 1. All neighboring *Inga* from the nine-focal species were included in this calculation including conspecifics. Roughly 52% of focal individuals had at least one conspecific neighbor within 10 meters with a mean total basal area of neighboring conspecifics of 710 mm^2. Focal individuals were far more

likely to have a congeneric neighbor with 87% of neighbors having at least one. The mean total

basal area of neighboring congenerics was 2610 mm^2.

We used a null model in our analysis to control for the fact that phylogenetic and trait

similarity vary with species richness (*6*, *7*, *24*, *28*, *68*). Thus, for each census interval we

obtained the expected mean similarity value for each trait by randomly swapping species labels

between all *Inga* in the plot. This null model was chosen because it retains spatial variation in

plot stem density as well as the clustered distribution of *Inga* congeners in the plot (Figure S5).

Note, however, that similar results were found when both species labels and the spatial

distribution of stems were randomized in the plot (Table S6). All observed trait values were

weighted using Equation S1 and trait similarity values represent the number of standard

deviations above or below the expected neighborhood similarity.

Equation S1:

$$\frac{Observed\ trait\ similarity\ -\ mean(null\ trait\ similarity)}{standard\ deviation(null\ trait\ simialrity)}$$

Focal tree growth was normalized within species, size class and census interval following

the methods of (*19*). Specifically, for each census interval we divided focal saplings into three

DBH classes delimited by diameters of 10, 30, and 50 mm. Each tree's normalized growth rate

is expressed as the number of positive or negative standard deviations by which the tree's growth

rate deviates from the mean growth rate of its size class within its species and census interval.

We constructed a separate mixed-effect model for conspecific density, congeneric

density, each of the nine trait similarity metrics as well as herbivore similarity using the R

package *LME4* (*69*). A linear mixed-effect model was used to model focal tree growth and a

logistic regression (family = "binomial") was used to model focal tree survival. Each model also

contained the percentage of neighboring individuals which were gap specialists as a random

intercept (1|Gap_density). Because species associated with high light environments often have specialized resource trait adaptations (*32*), we sought to confirm that the density of gap specialists was not correlated with the similarity of resource traits. Trait similarity was not associated with the percentage of individuals that were gap specialists (Figure S6), and thus the addition of gap specialists as a random effect should not influence the coefficients inferred for the resource acquisition traits in our models.

We also tested for spatial autocorrelations in our models using two methods: First, we added the identity of the quadrat (20m x 20m subplots within the larger 50-hectare plot) as well as the census interval as random effects in our models. We confirmed that this approach was sufficient to remove the spatial autocorrelation by checking for spatial autocorrelation within model residuals. Despite the fact that the original model residuals showed significant spatial autocorrelation (Moran's I statistic 0.020665, p= 0.001), models with these random effects showed no significant spatial autocorrelation (Moran's I statistic -0.00096297, p = 0.638). Our second approach involved creating spatial lag models using the function *lagsarlm* from the *spdep* R package (*70*), which incorporate a spatial weights matrix directly into one of the terms of the model in order to control for spatial autocorrelation. After controlling for spatial autocorrelation, we observed the same relationships between conspecific, congeneric and neighborhood trait similarities (Table S8) as those inferred from models not accounting for spatial autocorrelation (Figure 1, Table S8) and therefore conclude that spatial autocorrelation did not significantly impact our model interpretations.

Finally, we tested the sensitivity of the relationship between neighborhood similarity and focal tree growth and survival over larger distances by building the above-mentioned regression

models using a neighborhood radius of 25 meters instead of 10 m. We found that model

coefficients and interpretations did not change over this larger interval. (Table S2).

Table S1: Nine focal *Inga* (Fabaceae, Mimosoideae) species, their associated mean abundance across all eight census intervals and total number of individuals used in this analysis.

Species	Code	Mean Abundance	Total Number of Individuals
Inga cocleensis Pittier	ingaco	87	697
Inga laurina (Sw.)Willd.	ingafa	74	590
Inga goldmanii Pittier	ingago	406	3247
Inga marginata Willd.	ingama	756	6047
Inga pezizifera Benth.	ingape	174	1389
Inga nobilis Willd.	ingaqu	711	5690
Inga acuminata Benth.	ingas1	437	3494
Inga sapindoides Willd.	ingasa	310	2481
Inga umbellifera (Vahl) Steud.	ingaum	928	7430

Table S2. Relationship of neighborhood trait similarity with focal tree growth and survival calculated over a 25-meter radius. Models use linear and logistic regression models for growth and survival respectively.

A)	Estimate	Min (2.5 % CI)	Max (97.5% CI)	*P*	*P* Adjusted
Growth using a radius of 25 meters for the neighborhood analysis					
conspecific density	-0.0319	-0.0624	-0.0013	**0.0409**	0.45
congeneric density	0.0104	-0.0067	0.0275	0.2317	1.0000
defence: chemistry	-0.0347	-0.0653	-0.0041	**0.0259**	0.3106
defence: ants	-0.0031	-0.0231	0.017	0.7653	1.0000
defence: development	-0.0075	-0.029	0.0139	0.4906	1.0000
defence: hairs	0.0012	-0.0181	0.0206	0.9006	1.0000
defence: phenology	-0.0055	-0.0282	0.0172	0.634	1.0000
resource: wood density	-0.0033	-0.0255	0.0189	0.7684	1.0000
resource: elemental composition	-0.0023	-0.0246	0.02	0.8418	1.0000
resource: max height	-0.0075	-0.0329	0.018	0.5662	1.0000
resource: leaf morphology	-0.0279	-0.028	0.0168	0.6229	1.0000
herbivore similarity	-0.0428	-0.0566	0.0009	0.0572	0.5718
Survival using a radius of 25 meters for the neighborhood analysis					
conspecific density	-0.1445	-0.1883	-0.1027	**< 0.0001**	**< 0.0001**
congeneric density	0.0982	0.0592	0.1391	**< 0.0001**	**< 0.0001**
defence: chemistry	-0.0079	-0.1715	-0.088	**< 0.0001**	**< 0.0001**
defence: ants	-0.0158	-0.0437	0.0288	0.6667	1.0000
defence: development	-0.0052	-0.0527	0.0221	0.4075	1.0000
defence: hairs	-0.0244	-0.0412	0.0318	0.7784	1.0000
defence: phenology	-0.0095	-0.0627	0.0148	0.2165	1.0000
resource: wood density	-0.0347	-0.0481	0.0301	0.6336	1.0000
resource: elemental composition	-0.0221	-0.0712	0.0024	0.0638	0.5103
resource: max height	-0.0308	-0.0633	0.0202	0.2993	1.0000
resource: leaf morphology	-0.1176	-0.0682	0.0073	0.109	0.7633
herbivore similarity	-0.1524	-0.1583	-0.0783	**< 0.0001**	**< 0.0001**

Figure S1. Pair-wise comparison of trait similarity between *Inga* species. Below the diagonal represents a bivariate scatter plot of trait similarity with 36 points, one for each bidirectional comparison of *Inga* species. The diagonal represents a histogram of trait similarity. The R and P values above the diagonal represent the Pearson correlation and significance based on a Mantel test (10,000 iterations) respectively.

Table S3. Measures of phylogenetic signal for *Inga* traits. We used Blomberg´s K for each

Inga functional and defensive trait, the principal coordinates of the chemistry and phenology

similarity matrices (PCO), and principle components (PCA) of the leaf elemental composition.

For PCO and PCA values in parentheses represent the percentage of variation explained by each

component.

Defensive traits	K statistic	P (reps=9999)
Ants per Extrafloral Nectary	0.57	0.83
Chlorophyll Content	1.175	0.06
Trichome Density	0.86	0.56
Phenology PCO1 (37%)	0.68	0.7
Phenology PCO2 (19%)	0.68	0.7
Chemistry PCO1 (29%)	0.7	0.59
Chemistry PCO2 (20%)	0.55	0.95
Functional traits		
Wood Density	0.95	0.22
Elemental Composition PCA 1 (38%)	0.6	0.8
Elemental Composition PCA 2 (25%)	0.67	0.77
Average Height	0.72	0.58
Leaf Area	1.02	0.12

Table S4. Gap colonizing species used as a covariate to account for variation in light availability.

Species	Family	Code
Acalypha diversifolia Jacq.	Euphorbiaceae	acaldi
Alchornea costaricensis Pax & K. Hoffm.	Euphorbiaceae	alchco
Annona spraguei Saff.	Annonaceae	annosp
Apeiba tibourbou Aubl.	Malvaceae	apeiti
Cecropia insignis Liebm.	Urticaceae	cecrin
Cecropia longipes Pittier	Urticaceae	cecrlo
Cecropia obtusifolia Bertol.	Urticaceae	cecrob
Cordia bicolor A. DC.	Boraginaceae	cordbi
Croton billbergianus Müll. Arg.	Euphorbiaceae	crotbi
Hieronyma alchorneoides Allemão	Phyllanthaceae	hyeral
Jacaranda copaia (Aubl.) D. Don	Bignoniaceae	jac1co
Laetia thamnia L.	Salicaceae	laetth
Luehea seemannii Triana & Planch.	Malvaceae	luehse
Miconia argentea (Sw.) DC.	Melastomataceae	micoar
Ochroma pyramidale (Cav. ex Lam.) Urb.	Malvaceae	ochrpy
Ocotea cernua (Nees) Mez	Lauraceae	ocotce
Ocotea puberula (Rich.) Nees	Lauraceae	ocotpu
Trophis caucana (Pittier) C.C. Berg	Moraceae	olmeas
Palicourea guianensis Aubl.	Rubiaceae	paligu
Sapium glandulosum (L.) Morong	Euphorbiaceae	sapiau
Simarouba amara Aubl.	Simaroubaceae	simaam
Tabebuia rosea (Bertol.) DC.	Bignoniaceae	tab1ro
Trattinnickia aspera (Standl.) Swart	Burseraceae	tratas
Trema micrantha (L.) Blume	Cannabaceae	tremmi
Zuelania guidonia (Sw.) Britton & Millsp.	Salicaceae	zuelgu

Table S5: **Influence of conspecific density, density of gap specialists and the interaction between both covariates on normalized growth and survival.** Min and Max represent the 95% confidence intervals on the estimated effect sizes.

	Estimate	Min (2.5 % CI)	Max (97.5% CI)	P
Growth				
conspecificdensity	-0.0478374	0.08817613	-0.00749862	0.02
gap_density	0.005585	0.004843963	0.006326087	< 0.001
conspecificdensity*gap_density	0.0003132	-0.00105295	0.001679349	0.65
Survival				
conspecificdensity	-0.1508459	-0.20743819	-0.09849713	< 0.001
gap_density	-0.0121271	-0.01323948	-0.01102453	< 0.001
conspecificdensity*gap_density	0.0010751	-0.000520208	0.00254842	0.17

Table S6. Relationship between neighborhood trait similarity with focal tree growth and survival, using linear and logistic regression models, respectively. Model outputs are reported with and without density of gap specialist as a random effect. A) based on a spatially fixed null model where focal species labels are randomly swapped. B) based on null model where both tip labels and location of stems are randomly generated.

A) Spatially Fixed Null Model	Estimate	Min (2.5 % CI)	Max (97.5% CI)	*P*	*P* Adjusted
Growth with no random effect					
conspecific density	-0.0302	-0.0609	0.0005	0.0537	0.5910
congeneric density	0.0054	-0.0100	0.0208	0.4899	1.0000
defence: chemistry	-0.0319	-0.0626	-0.0011	**0.0423**	0.5077
defence: ants	-0.0052	-0.0234	0.0130	0.5732	1.0000
defence: development	-0.0072	-0.0286	0.0142	0.5093	1.0000
defence: hairs	0.0003	-0.0194	0.0199	0.9797	1.0000
defence: phenology	-0.0069	-0.0295	0.0157	0.5488	1.0000
resource: wood density	-0.0015	-0.0222	0.0192	0.8869	1.0000
resource: elemental composition	-0.0016	-0.0231	0.0199	0.8853	1.0000
resource: max height	-0.0048	-0.0298	0.0202	0.7071	1.0000
resource: leaf morphology	-0.0058	-0.0288	0.0173	0.6249	1.0000
herbivore similarity	-0.0267	-0.0554	0.0020	0.0679	0.6793
Growth with gap as random effect					
conspecific density	-0.0407	-0.0715	-0.0099	**0.0096**	0.1053
congeneric density	0.0025	-0.0129	0.0178	0.7531	1.0000
defence: chemistry	-0.0428	-0.0736	-0.0120	**0.0065**	0.0782
defence: ants	-0.0095	-0.0276	0.0087	0.3055	1.0000
defence: development	-0.0124	-0.0337	0.0090	0.2554	1.0000
defence: hairs	-0.0045	-0.0241	0.0150	0.6485	1.0000
defence: phenology	-0.0135	-0.0361	0.0090	0.2394	1.0000
resource: wood density	-0.0073	-0.0279	0.0134	0.4895	1.0000
resource: elemental composition	-0.0083	-0.0298	0.0132	0.4485	1.0000
resource: max height	-0.0123	-0.0372	0.0126	0.3340	1.0000
resource: leaf morphology	-0.0130	-0.0360	0.0100	0.2681	1.0000
herbivore similarity	-0.0370	-0.0658	-0.0083	**0.0116**	0.1155

Table S6: cont.

A) cont.	Estimate	Min (2.5 % CI)	Max (97.5% CI)	P	P Adjusted
Survival with no random effect					
conspecific density	-0.1445	-0.1911	-0.1010	**< 0.001**	**< 0.001**
congeneric density	0.0865	0.0510	0.1245	**< 0.001**	**< 0.001**
defence: chemistry	-0.1257	-0.1703	-0.0840	**< 0.001**	**< 0.001**
defence: ants	-0.0122	-0.0418	0.0185	0.4251	1.0000
defence: development	-0.0255	-0.0595	0.0092	0.1430	0.5722
defence: hairs	-0.0124	-0.0461	0.0224	0.4767	1.0000
defence: phenology	-0.0350	-0.0700	0.0005	0.0508	0.3559
resource: wood density	-0.0126	-0.0459	0.0218	0.4651	1.0000
resource: elemental composition	-0.0355	-0.0680	-0.0027	0.0321	0.2568
resource: max height	-0.0337	-0.0706	0.0039	0.0753	0.3847
resource: leaf morphology	-0.0335	-0.0687	0.0024	0.0641	0.3847
herbivore similarity	-0.1136	-0.1552	-0.0746	**< 0.001**	**< 0.001**
Survival with gap as random effect					
conspecific density	-0.1346	-0.1814	-0.0911	**< 0.001**	**< 0.001**
congeneric density	0.0978	0.0606	0.1374	**< 0.001**	**< 0.001**
defence: chemistry	-0.1158	-0.1606	-0.0741	**< 0.001**	**< 0.001**
defence: ants	-0.0045	-0.0355	0.0276	0.7766	1.0000
defence: development	-0.0174	-0.0528	0.0188	0.3389	1.0000
defence: hairs	-0.0029	-0.0382	0.0335	0.8728	1.0000
defence: phenology	-0.0253	-0.0617	0.0118	0.1762	1.0000
resource: wood density	-0.0030	-0.0378	0.0329	0.8673	1.0000
resource: elemental composition	-0.0266	-0.0603	0.0077	0.1245	0.9957
resource: max height	-0.0248	-0.0632	0.0144	0.2093	1.0000
resource: leaf morphology	-0.0232	-0.0599	0.0143	0.2191	1.0000
herbivore similarity	-0.1038	-0.1456	-0.0645	**< 0.001**	**< 0.001**

Table S6: cont.

B) Spatially Variable Null Model	Estimate	Min (2.5 % CI)	Max (97.5% CI)	P	P Adjusted
Growth with no random effect					
conspecific density	-0.0361	0.0188	0.0006	0.0541	0.595
congeneric density	0.0058	0.0085	0.0225	0.4956	1.0000
defence: chemistry	-0.0379	0.0187	-0.0013	**0.0426**	0.5117
defence: ants	-0.0061	0.0109	0.0152	0.5742	1.0000
defence: development	-0.0086	0.013	0.0168	0.5082	1.0000
defence: hairs	0.0002	0.0115	0.0228	0.9848	1.0000
defence: phenology	-0.0082	0.0137	0.0187	0.5499	1.0000
resource: wood density	-0.0018	0.0117	0.0212	0.8808	1.0000
resource: elemental composition	-0.002	0.0128	0.0232	0.8788	1.0000
resource: max height	-0.0053	0.014	0.0222	0.7031	1.0000
resource: leaf morphology	-0.0066	0.0133	0.0196	0.6223	1.0000
herbivore similarity	-0.0321	0.0176	0.0024	0.0683	0.683
Growth with gap as random effect					
conspecific density	-0.17	-0.2265	-0.1174	**< 0.001**	**< 0.001**
congeneric density	0.1	0.0603	0.1424	**< 0.001**	**< 0.001**
defence: chemistry	-0.1473	-0.2013	-0.0971	**< 0.001**	**< 0.001**
defence: ants	-0.011	-0.0468	0.0262	0.7766	1.0000
defence: development	-0.0265	-0.0681	0.0161	0.3389	0.8628
defence: hairs	-0.0112	-0.0513	0.0303	0.8728	1.0000
defence: phenology	-0.0378	-0.0808	0.0059	0.1762	0.6047
resource: wood density	-0.0106	-0.0487	0.0288	0.8673	1.0000
resource: elemental composition	-0.0388	-0.0779	0.0009	0.1245	0.4238
resource: max height	-0.0341	-0.076	0.0087	0.2093	0.6237
resource: leaf morphology	-0.0344	-0.0757	0.0076	0.2191	0.6237
herbivore similarity	-0.1337	-0.1844	-0.0861	**< 0.001**	**< 0.001**

Table S6: cont.

B) cont.	Estimate	Min (2.5 % CI)	Max (97.5% CI)	*P*	*P* Adjusted
Survival with no random effect					
conspecific density	-0.1711	-0.2268	-0.1191	**< 0.001**	**< 0.001**
congeneric density	0.0943	0.0557	0.1355	**< 0.001**	**< 0.001**
defence: chemistry	-0.1484	-0.2017	-0.0989	**< 0.001**	**< 0.001**
defence: ants	-0.0132	-0.0479	0.0228	0.4622	1
defence: development	-0.0288	-0.0691	0.0125	0.1649	0.6597
defence: hairs	-0.0131	-0.0519	0.027	0.5146	1
defence: phenology	-0.04	-0.0816	0.0024	0.0615	0.4305
resource: wood density	-0.0129	-0.0498	0.0252	0.4989	1
resource: elemental composition	-0.0404	-0.0783	-0.002	0.037	0.2963
resource: max height	-0.0358	-0.0764	0.0057	0.0864	0.4509
resource: leaf morphology	-0.0365	-0.0765	0.0042	0.0751	0.4509
herbivore similarity	-0.1352	-0.1852	-0.0883	**< 0.001**	**< 0.001**
Survival with gap as random effect					
conspecific density	-0.17	-0.2265	-0.1174	**< 0.001**	**< 0.001**
congeneric density	0.1	0.0603	0.1424	**< 0.001**	**< 0.001**
defence: chemistry	-0.1473	-0.2013	-0.0971	**< 0.001**	**< 0.001**
defence: ants	-0.011	-0.0468	0.0262	0.5534	1
defence: development	-0.0265	-0.0681	0.0161	0.2157	0.8628
defence: hairs	-0.0112	-0.0513	0.0303	0.59	1
defence: phenology	-0.0378	-0.0808	0.0059	0.0864	0.6047
resource: wood density	-0.0106	-0.0487	0.0288	0.5909	1
resource: elemental composition	-0.0388	-0.0779	0.0009	0.053	0.4238
resource: max height	-0.0341	-0.076	0.0087	0.1135	0.6237
resource: leaf morphology	-0.0344	-0.0757	0.0076	0.104	0.6237
herbivore similarity	-0.1337	-0.1844	-0.0861	**< 0.001**	**< 0.001**

Table S7. Proportion of saplings with herbivores, total number of herbivores collected and number of herbivore species (MOTU) per *Inga* species.

Species	Sapling with Herbivores	Saplings Sampled	Percent with Herbivores	Number of Herbivores Collected	Number of Herbivore Species (MOTU)
Inga cocleensis	21	50	42	69	13
Inga laurina	16	29	55	13	0
Inga goldmanii	20	46	43	62	12
Inga marginata.	47	121	39	65	16
Inga pezizifera.	34	67	51	67	4
Inga nobilis.	20	70	29	20	26
Inga acuminata.	21	105	20	23	35
Inga sapindoides.	20	55	36	36	19
Inga umbellifera	48	140	34	258	21
All study species	**247**	**683**	**36**	**613**	**55**

Figure S2: Herbivore community associated with nine focal *Inga* species. We collected 613

individuals sorted into 55 molecular operational taxonomic units from 24 families.
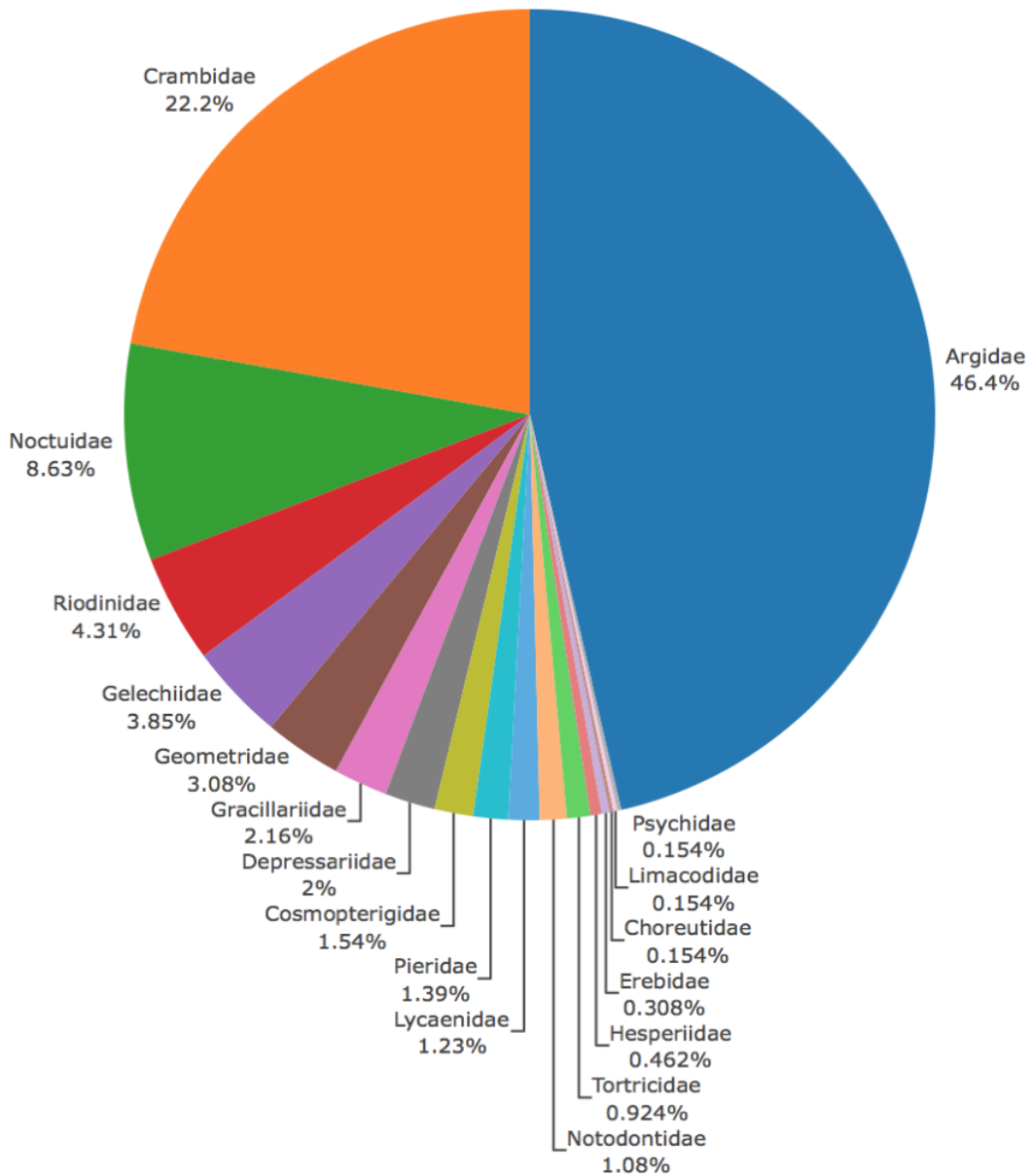
Figure S3: Frequency plot of the number of *Inga* hosts associated with each herbivore molecular operational taxonomic unit (MOTU).

Figure S4: Jaccard index of herbivore similarity between _Inga_ species.
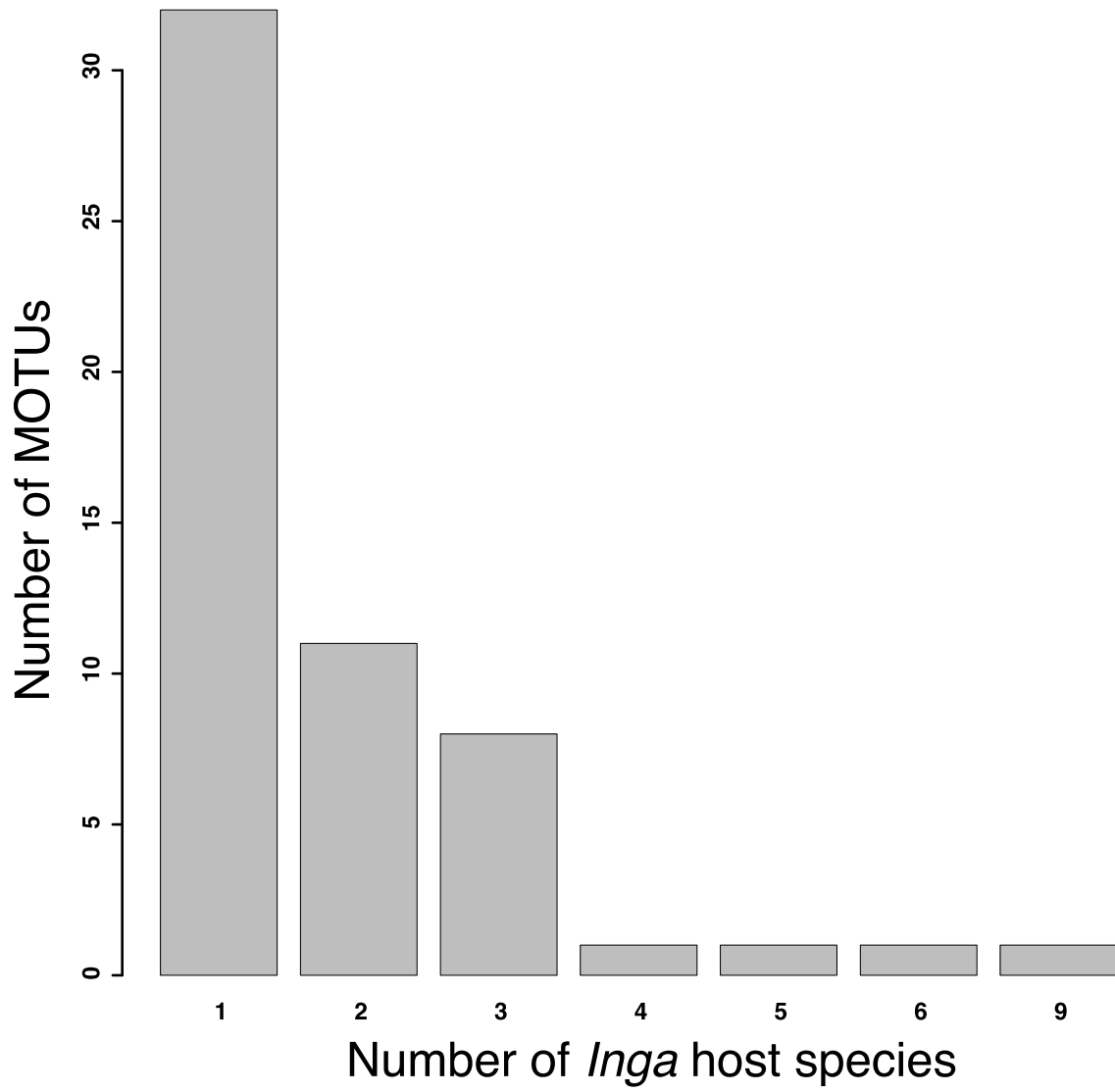
Figure S5: Density of *Inga* in the BCI 50-hectare plot at the start of each census interval.
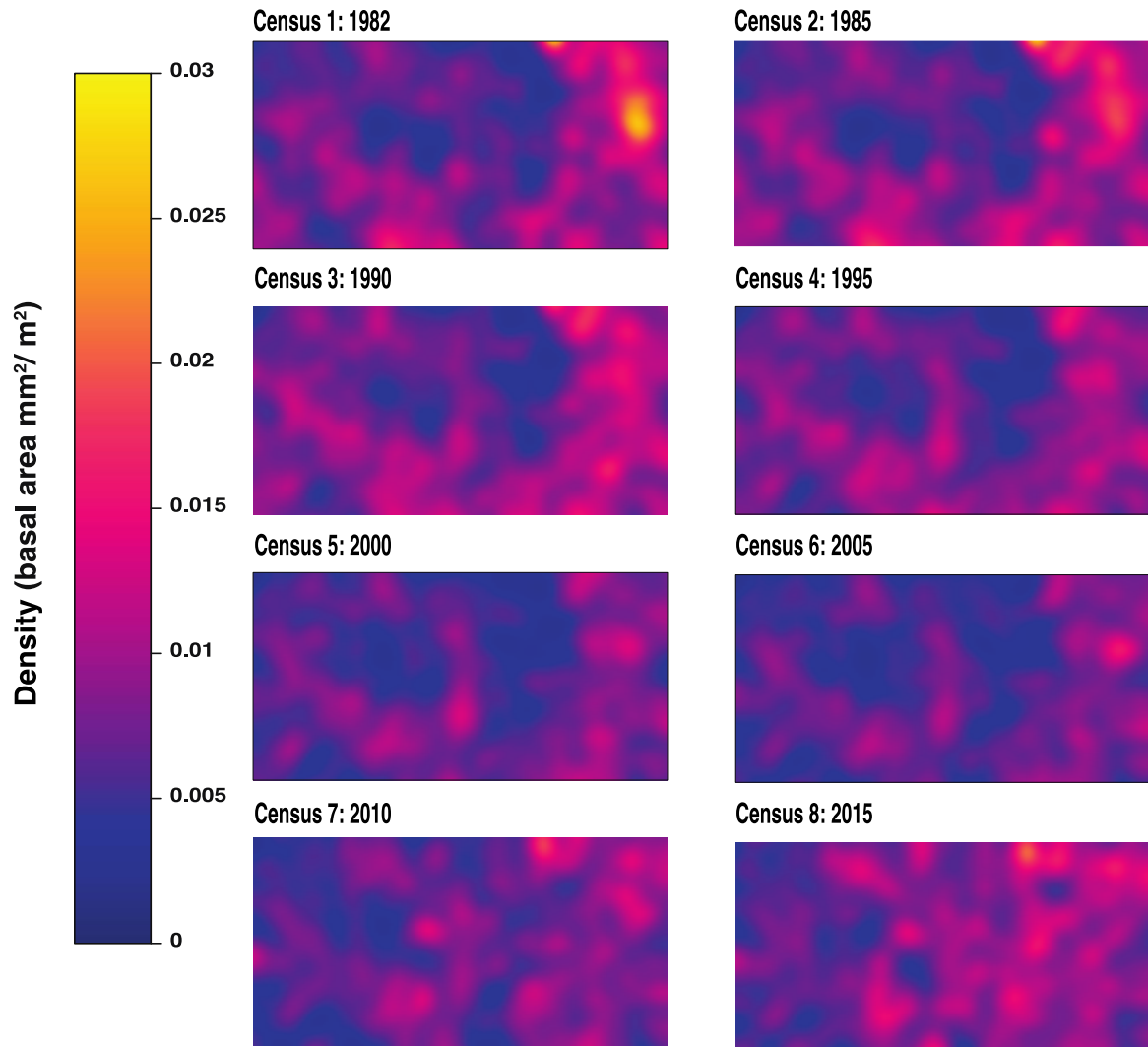
Figure S6: Relationship between the neighborhood trait similarity and the percentage of gap specialists for each focal tree.

Percentage of Neighbors that are Gap Specialist
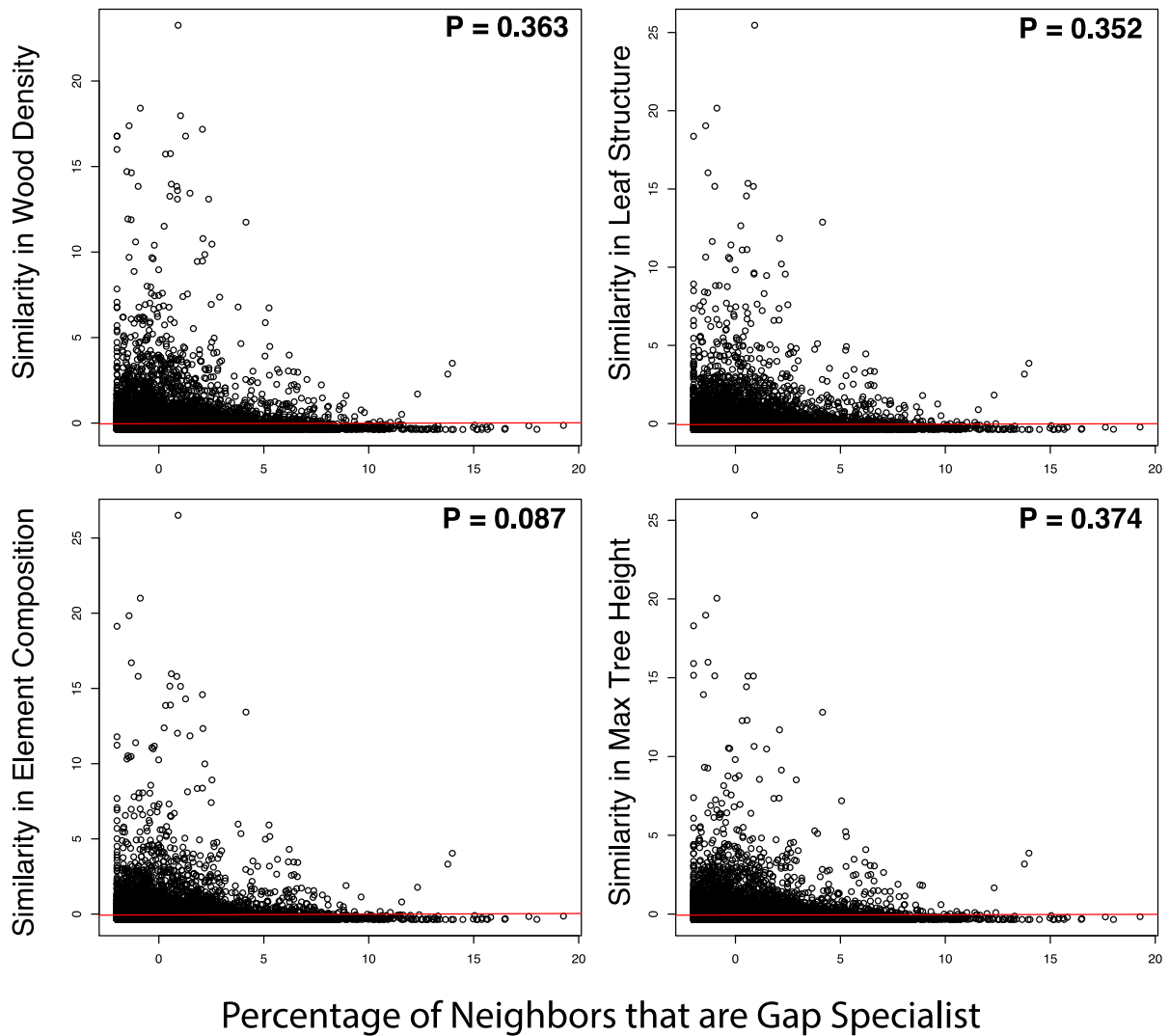
Table S8. Relationship between neighborhood trait similarity with focal tree growth and survival, using linear and logistic regression models, respectively. Models designed to account for spatial autocorrelation. A) Model built while including the quadrat identity as well as the census interval as random effects. B) Spatial lag model using the *lagsarlm* from the *spdep* R package (*69*).

A)

	Estimate	Min (2.5 % CI)	Max (97.5% CI)	*P*	*P* Adjusted
Growth with quadrat and census interval as random effect					
conspecific density	-0.0455	-0.0809	-0.01	**0.012**	0.1293
congeneric density	0.0008	-0.0148	0.0164	0.9177	1.0000
defence: chemistry	-0.0482	-0.084	-0.0124	**0.0083**	0.0994
defence: ants	-0.0109	-0.031	0.0093	0.2894	1.0000
defence: development	-0.0155	-0.0392	0.0083	0.2013	1.0000
defence: hairs	-0.0048	-0.0257	0.0161	0.6533	1.0000
defence: phenology	-0.0158	-0.0412	0.0096	0.2229	1.0000
resource: wood density	-0.0098	-0.0321	0.0125	0.3888	1.0000
resource: elemental composition	-0.0111	-0.0355	0.0132	0.3697	1.0000
resource: max height	-0.0172	-0.0444	0.0101	0.2157	1.0000
resource: leaf morphology	-0.0145	-0.0396	0.0106	0.2564	1.0000
herbivore similarity	-0.0428	-0.0761	-0.0095	**0.0118**	0.1293
Survival with quadrat and census interval as random effects					
conspecific density	-0.1365	-0.1915	-0.0853	**< 0.0001**	**< 0.0001**
congeneric density	0.106	0.0663	0.1485	**< 0.0001**	**< 0.0001**
defence: chemistry	-0.1188	-0.1725	-0.0685	**< 0.0001**	**0.0001**
defence: ants	0.0084	-0.0292	0.0476	0.6632	1.0000
defence: development	-0.0081	-0.0507	0.036	0.7135	1.0000
defence: hairs	0.0063	-0.0352	0.0493	0.7662	1.0000
defence: phenology	-0.02	-0.0645	0.0253	0.3817	1.0000
resource: wood density	0.0083	-0.0326	0.0507	0.6929	1.0000
resource: elemental composition	-0.0083	-0.06	0.0239	0.39	1.0000
resource: max height	-0.0217	-0.0669	0.0242	0.349	1.0000
resource: leaf morphology	-0.0152	-0.0589	0.0296	0.4979	1.0000
herbivore similarity	-0.1048	-0.1552	-0.057	**< 0.0001**	**0.0002**

Table S8. Cont.

B)	Estimate	Min (2.5 % CI)	Max (97.5% CI)	*P*	*P* Adjusted
Growth based on a spatial lag model					
conspecific density	-0.0455	-0.0793	-0.0117	**0.0084**	0.092
congeneric density	0.0016	-0.0128	0.0161	0.8226	1.0000
defence: chemistry	-0.0477	-0.0818	0.0087	**0.006**	0.0722
defence: ants	-0.01	-0.0287	0.0101	0.2932	1.0000
defence: development	-0.0119	-0.0338	0.0172	0.2886	1.0000
defence: hairs	-0.0022	-0.0215	0.0108	0.8262	1.0000
defence: phenology	-0.0127	-0.0362	0.0096	0.2892	1.0000
resource: wood density	-0.0075	-0.0281	0.0132	0.4777	1.0000
resource: elemental composition	-0.0084	-0.031	0.0142	0.4647	1.0000
resource: max height	-0.013	-0.0383	0.0122	0.312	1.0000
resource: leaf morphology	-0.0111	-0.0344	0.0122	0.3518	1.0000
herbivore similarity	-0.0412	-0.0726	-0.0097	**0.0104**	0.1038

References and Notes

1. R. Valencia, R. Condit, R. B. Foster, K. Romoleroux, G. V. Munoz, J.-C. Svenning, E. Magard, M. Bass, E. C. Losos, H. Balslev, in *Forest Diversity and Dynamism: Findings from a Large-Scale Plot Network*, E. C. Losos, E. G. Leigh, Eds. (Univ. of Chicago Press, 2004), pp. 609–620.

2. P. Chesson, Mechanisms of maintenance of species diversity. *Annu. Rev. Ecol. Syst.* **31**, 343–366 (2000). doi:10.1146/annurev.ecolsys.31.1.343

3. J. S. Wright, Plant diversity in tropical forests: A review of mechanisms of species coexistence. *Oecologia* **130**, 1–14 (2002). [doi:10.1007/s004420100809](doi:10.1007/s004420100809) Medline

4. J. Terborgh, Enemies maintain hyperdiverse tropical forests. *Am. Nat.* **179**, 303–314 (2012). [doi:10.1086/664183](doi:10.1086/664183) Medline

5. W. P. Carson, J. T. Anderson, E. G. J. Leigh, S. A. Schnitzer, in *Tropical Forest Community Ecology*, W. P. Carson, S. A. Schnitzer, Eds. (Wiley-Blackwell, 2008), pp. 210–241.

6. M. R. Metz, W. P. Sousa, R. Valencia, Widespread density-dependent seedling mortality promotes species coexistence in a highly diverse Amazonian rain forest. *Ecology* **91**, 3675–3685 (2010). [doi:10.1890/08-2323.1](doi:10.1890/08-2323.1) Medline

7. Y. Zhu, L. S. Comita, S. P. Hubbell, K. Ma, Conspecific and phylogenetic density-dependent survival differs across life stages in a tropical forest. *J. Ecol.* **103**, 957–966 (2015). [doi:10.1111/1365-2745.12414](doi:10.1111/1365-2745.12414)

8. R. Bagchi, T. Swinfield, R. E. Gallery, O. T. Lewis, S. Gripenberg, L. Narayan, R. P. Freckleton, Testing the Janzen-Connell mechanism: Pathogens cause overcompensating density dependence in a tropical tree. *Ecol. Lett.* **13**, 1262–1269 (2010). [doi:10.1111/j.1461-0248.2010.01520.x](doi:10.1111/j.1461-0248.2010.01520.x) Medline

9. R. Bagchi, R. E. Gallery, S. Gripenberg, S. J. Gurr, L. Narayan, C. E. Addis, R. P. Freckleton, O. T. Lewis, Pathogens and insect herbivores drive rainforest plant diversity and composition. *Nature* **506**, 85–88 (2014). doi:10.1038/nature12911 Medline

10. E. C. Fricke, J. J. Tewksbury, H. S. Rogers, Multiple natural enemies cause distance-dependent mortality at the seed-to-seedling transition. *Ecol. Lett.* **17**, 593–598 (2014). [doi:10.1111/ele.12261](doi:10.1111/ele.12261) Medline

11. J. Zambrano, Y. Iida, R. Howe, L. Lin, M. N. Umana, A. Wolf, S. J. Worthy, N. G. Swenson, Neighbourhood defence gene similarity effects on tree performance: A community transcriptomic approach. *J. Ecol.* **105**, 616–626 (2017). [doi:10.1111/1365-2745.12765](doi:10.1111/1365-2745.12765)

12. L. S. Comita, S. A. Queenborough, S. J. Murphy, J. L. Eck, K. Xu, M. Krishnadas, N. Beckman, Y. Zhu, L. Gómez-Aparicio, Testing predictions of the Janzen-Connell hypothesis: A meta-analysis of experimental evidence for distance- and density-dependent seed and seedling survival. *J. Ecol.* **102**, 845–856 (2014). [doi:10.1111/1365-2745.12232](doi:10.1111/1365-2745.12232) Medline

13. S. A. Mangan, S. A. Schnitzer, E. A. Herre, K. M. L. Mack, M. C. Valencia, E. I. Sanchez, J. D. Bever, Negative plant-soil feedback predicts tree-species relative abundance in a tropical forest. *Nature* **466**, 752–755 (2010). doi:10.1038/nature09273 Medline

14. P. T. Green, K. E. Harms, J. H. Connell, Nonrandom, diversifying processes are disproportionately strong in the smallest size classes of a tropical forest. *Proc. Natl. Acad. Sci. U.S.A.* **111**, 18649–18654 (2014). doi:10.1073/pnas.1321892112 Medline

15. D. H. Janzen, Herbivores and the number of tree species in tropical forests. *Am. Nat.* **104**, 501–528 (1970). doi:10.1086/282687

16. J. H. Connell, in *Dynamics of Populations*, vol. 298, P. J. den Boer, G. R. Gradwell, Eds. (Centre for Agricultural Publishing and Documentation, 1971), pp. 298–312.

17. P. D. Coley, M.-J. Endara, T. A. Kursar, Consequences of interspecific variation in defenses and herbivore host choice for the ecology and evolution of *Inga*, a speciose rainforest tree. *Oecologia* **187**, 361–376 (2018). doi:10.1007/s00442-018-4080-z Medline

18. K. G. Dexter, M. Lavin, B. M. Torke, A. D. Twyford, T. A. Kursar, P. D. Coley, C. Drake, R. Hollands, R. T. Pennington, Dispersal assembly of rain forest tree communities across the Amazon basin. *Proc. Natl. Acad. Sci. U.S.A.* **114**, 2645–2650 (2017). doi:10.1073/pnas.1613655114 Medline

19. C. Wills, K. E. Harms, T. Wiegand, R. Punchi-Manage, G. S. Gilbert, D. Erickson, W. J. Kress, S. P. Hubbell, C. V. Gunatilleke, I. A. Gunatilleke, Persistence of neighborhood demographic influences over long phylogenetic distances may help drive post-speciation adaptation in tropical forests. *PLOS ONE* **11**, e0156913 (2016). doi:10.1371/journal.pone.0156913 Medline

20. J. Cavender-Bares, D. D. Ackerly, D. A. Baum, F. A. Bazzaz, Phylogenetic overdispersion in Floridian oak communities. *Am. Nat.* **163**, 823–843 (2004). doi:10.1086/386375 Medline

21. N. G. Swenson, B. J. Enquist, Opposing assembly mechanisms in a neotropical dry forest: Implications for phylogenetic and functional community ecology. *Ecology* **90**, 2161–2170 (2009). doi:10.1890/08-1025.1 Medline

22. T. A. Kursar, K. G. Dexter, J. Lokvam, R. T. Pennington, J. E. Richardson, M. G. Weber, E. T. Murakami, C. Drake, R. McGregor, P. D. Coley, The evolution of antiherbivore defenses and their contribution to species coexistence in the tropical tree genus *Inga*. *Proc. Natl. Acad. Sci. U.S.A.* **106**, 18073–18078 (2009). doi:10.1073/pnas.0904786106 Medline

23. D. Salazar, M. A. Jaramillo, R. J. Marquis, Chemical similarity and local community assembly in the species rich tropical genus *Piper*. *Ecology* **97**, 3176–3183 (2016). doi:10.1002/ecy.1536 Medline

24. N. J. B. Kraft, R. Valencia, D. D. Ackerly, Functional traits and niche-based tree community assembly in an Amazonian forest. *Science* **322**, 580–582 (2008). doi:10.1126/science.1160662 Medline

25. See supplementary materials and methods.

26. M.-J. Endara, P. D. Coley, G. Ghabash, J. A. Nicholls, K. G. Dexter, D. A. Donoso, G. N. Stone, R. T. Pennington, T. A. Kursar, Coevolutionary arms race versus host defense chase in a tropical herbivore-plant system. *Proc. Natl. Acad. Sci. U.S.A.* **114**, E7499–E7505 (2017). doi:10.1073/pnas.1707727114 Medline

27. M.-J. Endara, J. A. Nicholls, P. D. Coley, D. L. Forrister, G. C. Younkin, K. G. Dexter, C. A. Kidner, R. T. Pennington, G. N. Stone, T. A. Kursar, Tracking of host defenses and

phylogeny during the radiation of neotropical Inga-feeding sawflies (Hymenoptera; Argidae). *Front. Plant Sci.* **9**, 1237 (2018). doi:10.3389/fpls.2018.01237 Medline

28. C. Fortunel, J. R. Lasky, M. Uriarte, R. Valencia, S. J. Wright, N. C. Garwood, N. J. B. Kraft, Topography and neighborhood crowding can interact to shape species growth and distribution in a diverse Amazonian forest. *Ecology* **99**, 2272–2283 (2018). doi:10.1002/ecy.2441 Medline

29. R. L. Chazdon, R. W. Pearcy, D. W. Lee, N. Fetcher, in *Tropical Forest Plant Ecophysiology*, S. S. Mulkey, R. L. Chazdon, A. P. Smith, Eds. (Chapman & Hall, 1996), pp. 1–55.

30. P. M. Vitousek, J. S. Denslow, Nitrogen and phosphorus availability in treefall gaps of a lowland tropical rainforest. *J. Ecol.* **74**, 1167–1178 (1986). doi:10.2307/2260241

31. J. S. Denslow, A. M. Ellison, R. E. Sanford, Treefall gap size effects on above- and below-ground processes in a tropical wet forest. *J. Ecol.* **86**, 597–609 (1998). doi:10.1046/j.1365-2745.1998.00295.x

32. S. J. Wright, K. Kitajima, N. J. B. Kraft, P. B. Reich, I. J. Wright, D. E. Bunker, R. Condit, J. W. Dalling, S. J. Davies, S. Díaz, B. M. J. Engelbrecht, K. E. Harms, S. P. Hubbell, C. O. Marks, M. C. Ruiz-Jaen, C. M. Salvador, A. E. Zanne, Functional traits and the growth-mortality trade-off in tropical trees. *Ecology* **91**, 3664–3674 (2010). doi:10.1890/09-2335.1 Medline

33. D. H. Janzen, Ecological characterization of Costa Rican dry forest caterpillar fauna. *Biotropica* **20**, 120–135 (1988). doi:10.2307/2388184

34. J. A. Barone, Host-specificity of folivorous insects in a moist tropical forest. *J. Anim. Ecol.* **67**, 400–409 (1998). doi:10.1046/j.1365-2656.1998.00197.x

35. V. Novotny, Y. Basset, S. E. Miller, R. L. Kitching, M. Laidlaw, P. Drozd, L. Cizek, Local species richness of leaf-chewing insects feeding on woody plants from one hectare of a lowland rainforest. *Conserv. Biol.* **18**, 227–237 (2004). doi:10.1111/j.1523-1739.2004.00293.x

36. M. L. Forister, V. Novotny, A. K. Panorska, L. Baje, Y. Basset, P. T. Butterill, L. Cizek, P. D. Coley, F. Dem, I. R. Diniz, P. Drozd, M. Fox, A. E. Glassmire, R. Hazen, J. Hrcek, J. P. Jahner, O. Kaman, T. J. Kozubowski, T. A. Kursar, O. T. Lewis, J. Lill, R. J. Marquis, S. E. Miller, H. C. Morais, M. Murakami, H. Nickel, N. A. Pardikes, R. E. Ricklefs, M. S. Singer, A. M. Smilanich, J. O. Stireman, S. Villamarín-Cortez, S. Vodka, M. Volf, D. L. Wagner, T. Walla, G. D. Weiblen, L. A. Dyer, The global distribution of diet breadth in insect herbivores. *Proc. Natl. Acad. Sci. U.S.A.* **112**, 442–447 (2015). doi:10.1073/pnas.1423042112 Medline

37. C. O. Webb, Exploring the phylogenetic structure of ecological communities: An example for rain forest trees. *Am. Nat.* **156**, 145–155 (2000). doi:10.1086/303378 Medline

38. J. Vleminckx, D. Salazar, C. Fortunel, I. Mesones, N. Dávila, J. Lokvam, K. Beckley, C. Baraloto, P. V. A. Fine, Divergent secondary metabolites and habitat filtering both contribute to tree species coexistence in the Peruvian Amazon. *Front. Plant Sci.* **9**, 836 (2018). doi:10.3389/fpls.2018.00836 Medline

39. R. D. Holt, M. B. Bonsall, Apparent competition. *Annu. Rev. Ecol. Evol. Syst.* **48**, 447–471 (2017). doi:10.1146/annurev-ecolsys-110316-022628

40. D. W. Schemske, G. G. Mittelbach, H. V. Cornell, J. M. Sobel, K. Roy, Is there a latitudinal gradient in the importance of biotic interactions? *Annu. Rev. Ecol. Evol. Syst.* **40**, 245–269 (2009). doi:10.1146/annurev.ecolsys.39.110707.173430

41. ForestGEO Data Portal; http://ctfs.si.edu/datarequest/.

42. D. L. Forrister, Data for Forrister *et al.* 2019, Herbivores as drivers of NDD, Zenodo (2019); doi:10.5281/zenodo.2571716.

43. D. L. Forrister, Data for Forrister *et al.* 2019, Herbivores as drivers of NDD, GitHub (2019); https://github.com/dlforrister/Forrister_et_al_2019_Herbivores_as_drivers_of_NDD.git.

44. E. G. J. Leigh, in *Tropical Forest Ecology: A View from Barro Colorado Island* (Oxford Univ. Press, 1999), pp. 46–63.

45. S. P. Hubbell, R. Condit, R. B. Foster, Barro Colorado Forest Census Plot Data (2010); http://ctfs.si.edu/webatlas/datasets/bci.

46. R. Condit, *Tropical Forest Census Plots* (Springer-Verlag, 1998).

47. S. P. Hubbell, R. B. Foster, S. T. O'Brien, K. E. Harms, R. Condit, B. Wechsler, S. J. Wright, S. Loo de Lao, Light-gap disturbances, recruitment limitation, and tree diversity in a neotropical forest. *Science* **283**, 554–557 (1999). doi:10.1126/science.283.5401.554 Medline

48. R. Condit, S. Lao, R. Pérez, S. B. Dolins, R. B. Foster, S. P. Hubbell, Barro Colorado Forest Census Plot Data, Version 2012, Center for Tropical Forest Science Databases (2012); doi:10.5479/data.bci.20130603.

49. J. W. Westbrook, K. Kitajima, J. G. Burleigh, W. J. Kress, D. L. Erickson, S. J. Wright, What makes a leaf tough? Patterns of correlated evolution between leaf toughness traits and demographic rates among 197 shade-tolerant woody species in a neotropical forest. *Am. Nat.* **177**, 800–811 (2011). doi:10.1086/659963 Medline

50. T. M. Aide, Herbivory as a selective agent on the timing of leaf production in a tropical understory community. *Nature* **336**, 574–575 (1988). doi:10.1038/336574a0

51. T. M. Aide, Patterns of leaf development and herbivory in a tropical understory community. *Ecology* **74**, 455–466 (1993). doi:10.2307/1939307

52. L. P. C. Morellato, I. L. Hudson, M. R. Keatley, in *Phenological Research*, I. L. Hudson, M. R. Keatley, Eds. (Springer, 2010), pp. 339–359.

53. C. Agostinelli, U. Lund, R package "circular": Circular statistics (version 0.4-93) (2017).

54. A. A. Agrawal, Induced responses to herbivory in wild radish: Effects on several herbivores and plant fitness. *Ecology* **80**, 1713–1723 (1999). doi:10.1890/0012-9658(1999)080[1713:IRTHIW]2.0.CO;2

55. N. L. Wiggins, D. L. Forrister, M. J. Endara, P. D. Coley, T. A. Kursar, Quantitative and qualitative shifts in defensive metabolites define chemical defense investment during leaf development in *Inga*, a genus of tropical trees. *Ecol. Evol.* **6**, 478–492 (2016). doi:10.1002/ece3.1896 Medline

56. R. De Maesschalck, D. Jouan-Rimbaud, D. L. Massart, The Mahalanobis distance. *Chemometr. Intell. Lab. Syst.* **50**, 1–18 (2000). doi:10.1016/S0169-7439(99)00047-7

57. C. A. Smith, E. J. Want, G. O'Maille, R. Abagyan, G. Siuzdak, XCMS: Processing mass spectrometry data for metabolite profiling using nonlinear peak alignment, matching, and identification. *Anal. Chem.* **78**, 779–787 (2006). [doi:10.1021/ac051437y](https://doi.org/10.1021/ac051437y) [Medline]

58. C. Kuhl, R. Tautenhahn, C. Böttcher, T. R. Larson, S. Neumann, CAMERA: An integrated strategy for compound spectra extraction and annotation of liquid chromatography/mass spectrometry data sets. *Anal. Chem.* **84**, 283–289 (2012). [doi:10.1021/ac202450g](https://doi.org/10.1021/ac202450g) [Medline]

59. M.-J. Endara, P. D. Coley, N. L. Wiggins, D. L. Forrister, G. C. Younkin, J. A. Nicholls, R. T. Pennington, K. G. Dexter, C. A. Kidner, G. N. Stone, T. A. Kursar, Chemocoding as an identification tool where morphological- and DNA-based methods fall short: *Inga* as a case study. *New Phytol.* **218**, 847–858 (2018). [doi:10.1111/nph.15020](https://doi.org/10.1111/nph.15020) [Medline]

60. M. Wang, J. J. Carver, V. V. Phelan, L. M. Sanchez, N. Garg, Y. Peng, D. D. Nguyen, J. Watrous, C. A. Kapono, T. Luzzatto-Knaan, C. Porto, A. Bouslimani, A. V. Melnik, M. J. Meehan, W.-T. Liu, M. Crüsemann, P. D. Boudreau, E. Esquenazi, M. Sandoval-Calderón, R. D. Kersten, L. A. Pace, R. A. Quinn, K. R. Duncan, C.-C. Hsu, D. J. Floros, R. G. Gavilan, K. Kleigrewe, T. Northen, R. J. Dutton, D. Parrot, E. E. Carlson, B. Aigle, C. F. Michelsen, L. Jelsbak, C. Sohlenkamp, P. Pevzner, A. Edlund, J. McLean, J. Piel, B. T. Murphy, L. Gerwick, C.-C. Liaw, Y.-L. Yang, H.-U. Humpf, M. Maansson, R. A. Keyzers, A. C. Sims, A. R. Johnson, A. M. Sidebottom, B. E. Sedio, A. Klitgaard, C. B. Larson, C. A. B. P, D. Torres-Mendoza, D. J. Gonzalez, D. B. Silva, L. M. Marques, D. P. Demarque, E. Pociute, E. C. O'Neill, E. Briand, E. J. N. Helfrich, E. A. Granatosky, E. Glukhov, F. Ryffel, H. Houson, H. Mohimani, J. J. Kharbush, Y. Zeng, J. A. Vorholt, K. L. Kurita, P. Charusanti, K. L. McPhail, K. F. Nielsen, L. Vuong, M. Elfeki, M. F. Traxler, N. Engene, N. Koyama, O. B. Vining, R. Baric, R. R. Silva, S. J. Mascuch, S. Tomasi, S. Jenkins, V. Macherla, T. Hoffman, V. Agarwal, P. G. Williams, J. Dai, R. Neupane, J. Gurr, A. M. C. Rodríguez, A. Lamsa, C. Zhang, K. Dorrestein, B. M. Duggan, J. Almaliti, P.-M. Allard, P. Phapale, L.-F. Nothias, T. Alexandrov, M. Litaudon, J.-L. Wolfender, J. E. Kyle, T. O. Metz, T. Peryea, D.-T. Nguyen, D. VanLeer, P. Shinn, A. Jadhav, R. Müller, K. M. Waters, W. Shi, X. Liu, L. Zhang, R. Knight, P. R. Jensen, B. Ø. Palsson, K. Pogliano, R. G. Linington, M. Gutiérrez, N. P. Lopes, W. H. Gerwick, B. S. Moore, P. C. Dorrestein, N. Bandeira, Sharing and community curation of mass spectrometry data with Global Natural Products Social Molecular Networking. *Nat. Biotechnol.* **34**, 828–837 (2016). [doi:10.1038/nbt.3597](https://doi.org/10.1038/nbt.3597) [Medline]

61. B. E. Sedio, J. C. Rojas Echeverri, C. A. Boya P., S. J. Wright, Sources of variation in foliar secondary chemistry in a tropical forest tree community. *Ecology* **98**, 616–623 (2017). [doi:10.1002/ecy.1689](https://doi.org/10.1002/ecy.1689) [Medline]

62. N. V. Ivanova, J. R. Dewaard, P. D. N. Hebert, An inexpensive, automation-friendly protocol for recovering high-quality DNA. *Mol. Ecol. Notes* **6**, 998–1002 (2006). [doi:10.1111/j.1471-8286.2006.01428.x](https://doi.org/10.1111/j.1471-8286.2006.01428.x)

63. J. R. DeWaard, N. V. Ivanova, M. Hajibabaei, P. D. N. Hebert, in *Methods in Molecular Biology: Environmental Genetics*, C. Martin, Ed. (Humana Press, 2008), pp. 275–293.

64. R. C. Edgar, MUSCLE: Multiple sequence alignment with high accuracy and high throughput. *Nucleic Acids Res.* **32**, 1792–1797 (2004). [doi:10.1093/nar/gkh340](https://doi.org/10.1093/nar/gkh340) [Medline]

65. M. Jones, A. Ghoorah, M. Blaxter, jMOTU and Taxonerator: Turning DNA Barcode sequences into annotated operational taxonomic units. *PLOS ONE* **6**, e19259 (2011). doi:10.1371/journal.pone.0019259 Medline

66. N. Puillandre, A. Lambert, S. Brouillet, G. Achaz, ABGD, Automatic Barcode Gap Discovery for primary species delimitation. *Mol. Ecol.* **21**, 1864–1877 (2012). doi:10.1111/j.1365-294X.2011.05239.x Medline

67. J. Oksanen, F. G. Blanchet, M. Friendly, R. Kindt, P. Legendre, D. McGlinn, P. R. Minchin, R. B. O'Hara, G. L. Simpson, P. Solymos, M. H. H. Stevens, E. Szoecs, H. Wagner, Vegan: Community Ecology R package, version 2.5.3 (2018); cran.r-project.org/web/packages/vegan/vegan.pdf [accessed 15 December 2018].

68. N. G. Swenson, *Functional and Phylogenetic Ecology in R* (Springer, 2014).

69. D. Bates, M. Mächler, B. Bolker, S. Walker, Fitting linear mixed-effects models using lme4. *J. Stat. Softw.* **67**, 1–48 (2015). doi:10.18637/jss.v067.i01

70. R. Bivand, M. Altman, L. Anselin, R. Assunção, O. Berke, Spatial Dependence: Weighting Schemes, Statistics and Models (2017); https://r-forge.r-project.org/projects/spdep/.